Separation Science and Technology
Publication details, including instructions for authors and subscription information:
http://www.informaworld.com/smpp/title~content=t713708471

The Separation of Particulates from Supercritical Water Oxidation Processes

P. C. Dell'orco[a]; L. Li[a]; E. F. Gloyna[a]
[a] Environmental and Water Resources Engineering The University of Texas at Austin, Austin, Texas

To cite this Article Dell'orco, P. C. , Li, L. and Gloyna, E. F.(1993) 'The Separation of Particulates from Supercritical Water Oxidation Processes', Separation Science and Technology, 28: 1, 625 — 642
To link to this Article: DOI: 10.1080/01496399308019511
URL: http://dx.doi.org/10.1080/01496399308019511

SEPARATION SCIENCE AND TECHNOLOGY, 28(1-3), pp. 625-642 (1993)

THE SEPARATION OF PARTICULATES FROM SUPERCRITICAL WATER OXIDATION PROCESSES

P. C. Dell'Orco, L. Li, and E. F. Gloyna
Environmental and Water Resources Engineering
The University of Texas at Austin
Austin, Texas 78712

ABSTRACT

Small hydrocyclones with batch underflow receivers were assessed for their ability to separate micron-sized particulates from near-critical water solutions. Such particulates are expected from the effluent of a supercritical water oxidation reactor. The separation of micron-sized quartz silica, zirconia, and titania particles was investigated. An empirical expression was developed for the prediction of gross removal efficiencies as a function of a Stokes' number. Particle size distributions provided grade efficiencies for all experiments, and from these data, cut sizes were determined. Gross efficiencies up to 99% were observed for zirconia; cut sizes (d_{90} and d_{95}) near one micron were measured.

INTRODUCTION

Supercritical water oxidation (SCWO) is an innovative process for treating wastewaters and sludges. The process involves the oxidation of organic matter in water above its critical point (374.2°C, 22.1 MPa), and results in high destruction efficiencies of organic components in relatively short residence times (1,2).

At supercritical conditions, water possesses solvent characteristics that are different from those exhibited at room temperature and atmospheric pressure. At typical SCWO operating conditions, the dielectric constant of water is reduced below ten (3), water ion products less than 10^{-20} are observed (4), and hydrogen bonding is substantially reduced (5). These changes in solvent characteristics result in enhanced solubility and miscibility of gases (6) and hydrocarbons (7), and substantially reduced solubilities of electrolytes (8,9).

Due to reduced salt solubilities, the formation of metal oxides, and the presence of stable solid matter, particulates are present in the SCWO process. These particulates can cause equipment fouling and erosion. In addition, salts and solid matter may require removal for regulatory reasons. The reduced solubility of salts at supercritical conditions introduces the possibility for a solid-fluid separation. As a result, effective solid and salt removal at supercritical conditions is desirable both operationally and for the safe disposal of the effluent.

The separation of solids from water at elevated temperatures and pressures has received relatively little attention. Early studies for the removal of fission products from homogeneous nuclear reactor cycles examined the use of small hydrocyclones with underflow receivers (10,11). More recently, solids separation for microgravity separation applications in the SCWO process have been evaluated by Killilea, et al. (12), who studied a hydrocyclone and an impingement/filtration apparatus. An evaluation of several potential processes, as well as a characterization of SCWO ash, has been presented by Dell'Orco (13). Armellini and Tester have studied nucleation phenomena of simple electrolytes in supercritical water solutions (14). Thus, to date, research on solid-fluid separation under SCWO environments has been general and not conducive to engineering design of a full-scale separation system.

The objective of this research was to develop engineering design parameters for a solids separator operating in the critical regime. Specifically, two hydrocyclones, 10 mm and 25.4 mm in diameter, with underflow receivers were evaluated for their ability to remove particulates of known size distributions from water at subcritical and supercritical conditions. These particulates were of similar size to those resulting from the SCWO of wastewaters and sludges.

EXPERIMENTAL

The apparatus used for particle separation experiments is shown in Figure 1. Influent water and particles were fed with a high pressure diaphragm pump. The pressurized mixture passed through a mass flowmeter, through the tube side of two tube and shell heat exchangers (heated by the effluent), and into a tubular

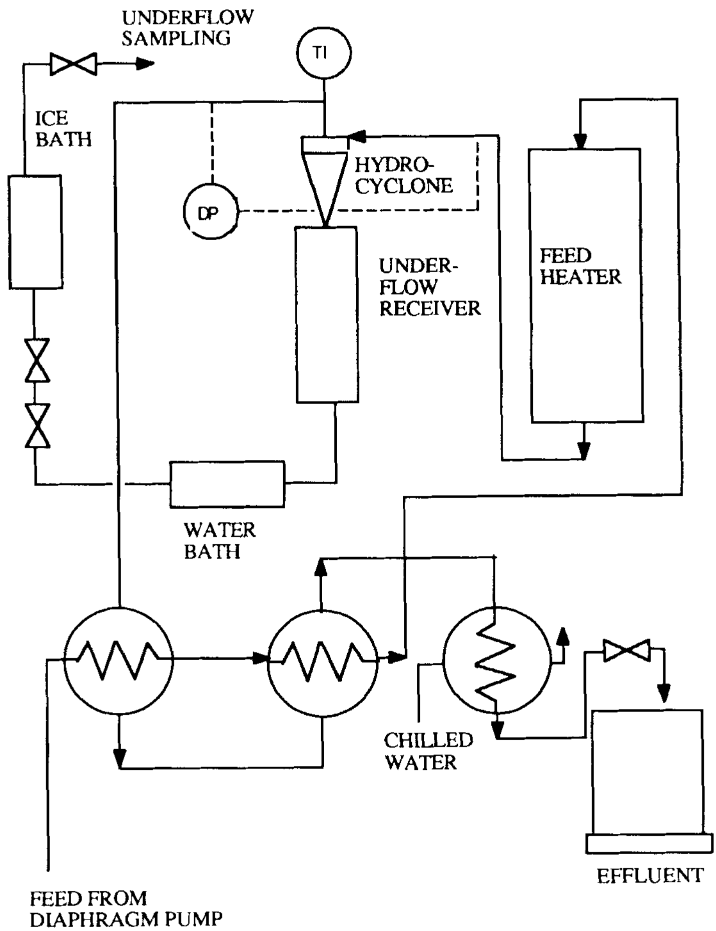

FIGURE 1. Solids separation apparatus.

heater. After exiting the heater, the fluid entered the hydrocyclone. Differential pressure from the feed entrance to the overflow exit was measured with a differential pressure transducer. Temperature was measured at the hydrocyclone overflow port with an Inconel sheathed, type K thermocouple. The overflow from the hydrocyclone was cooled by heat exchange with the feed, and by a final chilled water heat exchanger. From this final heat exchanger, the stream went through a pressure reduction valve, where it was sampled and continously collected. For a temperature and a pressure, three flow rates were used. Each flow rate was sustained for 10 to 15 minutes. The feed stream was then switched to water, and the underflow receiver was drained. Draining the underflow receiver consisted of metering the underflow stream while maintaining system pressure with the back-pressure regulating valve. Feed samples were taken at the beginning and end of experiments.

Hydrocyclone dimensions used are shown in Figure 2. The hydrocyclones share the same dimensional ratios of U/D, F/D, and O/D. Both also have circular, tangential feed ports. For the 10 mm diameter hydrocyclone (hydrocyclone A), the underflow receiver consisted of a 0.50 L high-pressure stainless steel cylinder which connected to the underflow port with an adapter fitting. The 25.4 mm diameter hydrocyclone (hydrocyclone B) had a 3.78 L underflow receiver which consisted of pipe (5.08 cm ID) flanged to the bottom of the hydrocyclone.

Feed, overflow stream, and underflow receiver samples were collected for the experiments. Sample volumes were measured in graduated cylinders. Each sample was measured for total solids, and diluted immediately for particle size distribution analyses. Particle size analyses were performed with a Coulter counter.

RESULTS AND DISCUSSION

Solids separation studies were conducted near 24.8 MPa at temperatures from 20°C to 400°C. Three different particle types were used: quartz silica (SiO_2, Min-U-Sil 5, U.S. Silica, Inc.), zirconia (ZrO_2, Zirox 360, Tam Ceramics), and titanium dioxide (TiO_2,Ti-Pure, E.I. du Pont de Nemours & Co., Inc.). Mass median particle diameters (d_{pm}) were measured with the Coulter counter to be 1.95, 3.45, and 2.10 µm, respectively. The mass median particle diameter was that diameter for which 50% of the mass was contained in particles with larger and smaller diameters. Particle specific gravities were 2.66 for silica, 5.60 for zirconia, and 3.60 for titania. Feed concentrations ranged from 400 mg/L to 1200 mg/L. From total solids data, gross efficiencies were calculated. Cut sizes were determined from grade efficiency curves, which were prepared from particle size distribution data. Pressure drop across the hydrocyclones was also measured.

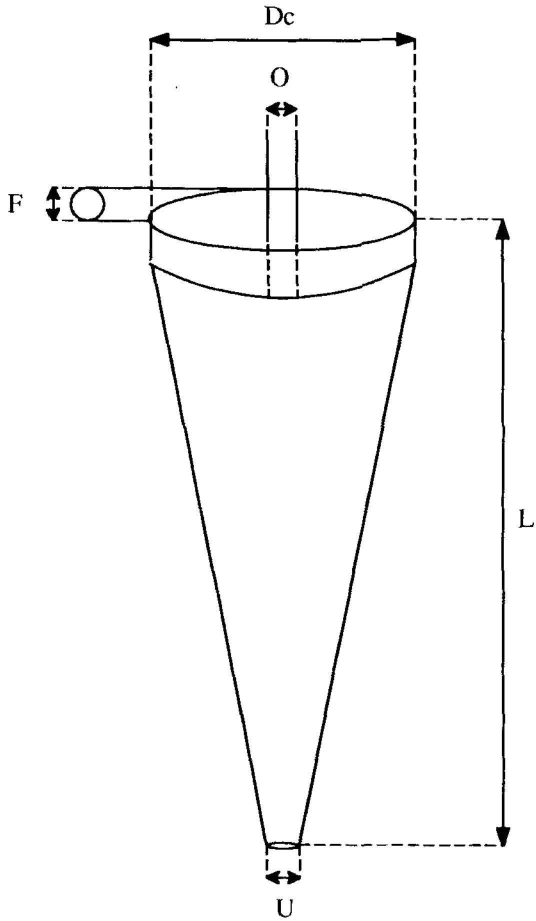

Hydrocyclone	Dc (mm)	L (mm)	F (mm)	U (mm)	O (mm)
A	10.00	54.10	2.95	2.50	2.50
B	25.40	145.80	7.49	6.35	6.35

FIGURE 2. Hydrocyclone dimensions.

Gross Removal Efficiencies

A summary of experimental conditions and gross removal efficiencies is shown in Table 1. The gross efficiency is defined by Eq. 1:

$$E_G = \frac{G_U}{G_F} \tag{1}$$

where

G_U	=	Mass flow rate of solids to underflow receiver, kg/s
G_F	=	Mass flow rate of solids in feed stream, kg/s.

Gross removal efficiencies for both hydrocyclones and all particulate feeds are shown in Figure 2. The figure plots penetration (1 - E_G) versus a dimensionless Stokes' number, represented by Eq. 2:

$$St = \frac{d_{pm}^2 * v_i * (\rho_p - \rho_w)}{9 * \mu * D_c} \tag{2}$$

where

St	=	Stokes' number, dimensionless
d_{pm}	=	mass median particle diameter, m
v_i	=	fluid velocity at feed port, m/s
ρ_p, ρ_w	=	density of particle, water, kg/m^3
μ	=	viscosity, kg/m*s
D_c	=	hydrocyclone diameter at feed port, m.

This particular Stokes' number, with modifications added for water systems, was adopted from Parker et al. (15), who used it to model efficiency data for air cyclones operating at elevated temperatures and pressures. Their Stokes' number also included a Cunningham slip factor, and did not account for the fluid density, since air densities were much smaller than particle densities in the study. The unique feature of this particular Stokes' number is the use of the mass median particle diameter as the characteristic particle diameter. This diameter is a bulk property of a particulate feed stream, determined from particle size distribution analyses. This Stokes' number was also used by Patterson and Munz (16) to represent efficiency data for air cyclones.

TABLE 1. EXPERIMENTAL CONDITIONS AND RESULTS

Expt.	Feed	Hydro-cylcone	Flow (kg/s)	Temp. (°C)	Press. (MPa)	C_{Feed} (mg/L)	E_G (%)
4S-1	SILICA	A	0.027	70	24.8	1071	11.4
4S-2	SILICA	A	0.037	70	24.8	1071	14.6
4S-3	SILICA	A	0.047	70	24.8	1071	20.0
4T-1	SILICA	A	0.027	78	24.8	670	15.8
4T-2	SILICA	A	0.037	78	24.8	670	22.7
4T-3	SILICA	A	0.047	80	24.8	670	31.5
5T-1	SILICA	A	0.027	147	24.8	667	44.8
5T-2	SILICA	A	0.037	147	24.8	667	44.4
5T-3	SILICA	A	0.047	161	24.8	667	41.4
5S-1	SILICA	A	0.030	211	24.8	1048	31.4
5S-2	SILICA	A	0.034	205	24.8	1048	24.1
5S-3	SILICA	A	0.044	213	24.8	1048	15.3
8T-1	SILICA	A	0.028	213	24.1	948	74.4
8T-2	SILICA	A	0.038	214	24.1	948	66.5
8T-3	SILICA	A	0.046	180	24.1	948	63.1
6S-1	SILICA	A	0.027	301	24.8	1229	72.5
6S-2	SILICA	A	0.037	292	24.8	1229	74.5
6S-3	SILICA	A	0.048	250	24.8	1229	81.0
12T-1	SILICA	A	0.012	389	24.1	923	81.5
12T-2	SILICA	A	0.022	369	24.1	923	81.5
12T-3	SILICA	A	0.028	371	24.1	923	81.6
6T-1	TITANIA	A	0.027	153	24.1	830	53.7
6T-2	TITANIA	A	0.037	150	24.1	830	53.2
6T-3	TITANIA	A	0.047	150	24.1	830	56.1
7T-1	TITANIA	A	0.028	243	24.1	681	93.4
7T-2	TITANIA	A	0.038	215	24.1	681	92.5
7T-3	TITANIA	A	0.048	216	24.1	681	95.9
9T-1	ZIRCONIA	A	0.028	217	25.5	525	88.8
9T-2	ZIRCONIA	A	0.038	216	25.5	525	93.3
9T-3	ZIRCONIA	A	0.046	217	25.5	525	70.7
10T-1	ZIRCONIA	A	0.028	280	25.5	826	93.4
10T-2	ZIRCONIA	A	0.037	252	25.5	826	92.5
10T-3	ZIRCONIA	A	0.045	252	25.5	826	95.9
11T-1	ZIRCONIA	A	0.018	280	24.8	461	99.2
11T-2	ZIRCONIA	A	0.024	275	24.8	461	97.2
11T-3	ZIRCONIA	A	0.028	252	24.8	461	99.5
13T-1	ZIRCONIA	A	0.013	370	24.8	522	88.8
13T-2	ZIRCONIA	A	0.019	378	24.8	522	93.3
13T-3	ZIRCONIA	A	0.028	360	24.8	522	70.7
L-2	SILICA	B	0.021	394	24.8	1042	71.0
L-3	SILICA	B	0.021	391	24.8	1042	76.9
L-4	SILICA	B	0.021	386	24.8	1042	69.3
L-5	SILICA	B	0.021	391	24.8	1042	76.5
L-7	SILICA	B	0.025	398	24.8	1042	75.8
L-8	SILICA	B	0.028	388	24.8	1042	76.2
L-9	SILICA	B	0.028	381	24.8	1042	70.6

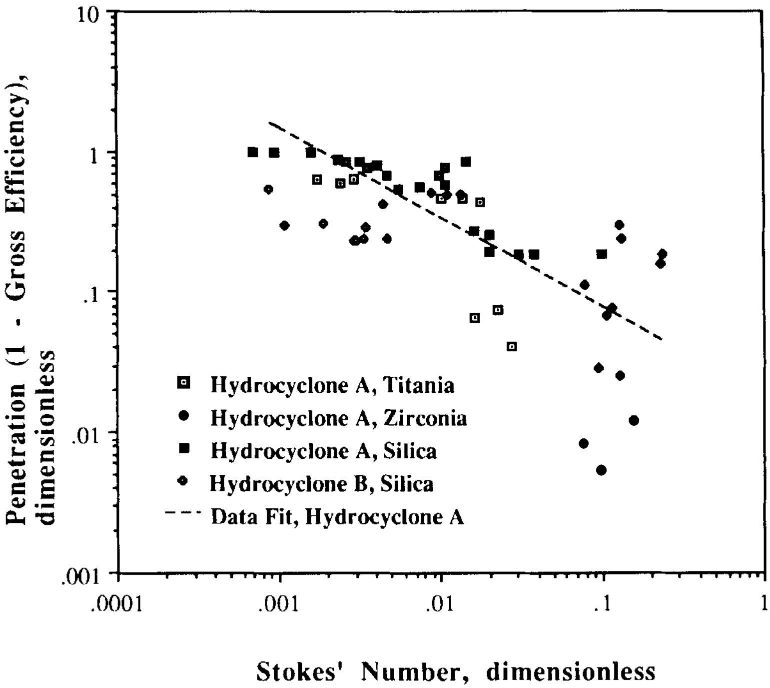

FIGURE 3. Gross efficiencies (as penetration) for all experiments.

For hydrocyclone A, Figure 3 shows increasing particulate removal with increases in the Stokes' number. This result is intuitively correct since the Stokes' number represents a ratio of centrifugal to inertial forces. Higher values of the Stokes' number represent a greater driving force for particulate removal. While the ln(Penetration) appears to vary linearly with ln(St) for hydrocyclone A, significant scatter is evident at high removal efficiencies. Most scatter was observed when high separations occurred at relatively low Stokes' numbers for zirconia.

For both hydrocyclones, silica approached a maximum gross efficiency near 80%. This limit may have developed due to the solubilization of some silica at elevated temperatures. Silica undergoes solubility changes over the temperature ranges encountered in this study (9), although the dissolution rate is believed to be slow (17). Without available *in situ* particle size distribution measurement techniques, the extent of solubilization and recrystallization, and their effects on removal efficiencies, was unknown. Removal efficiencies as high as 99% and 95% were observed for zirconia and titania particulates, respectively.

Removal efficiencies observed for hydrocyclones A and B did not follow the same trends. Removal efficiencies near 80% for silica attained with hydrocyclone B required Stokes' numbers 1-2 orders of magnitude lower than for the same removal efficiencies achieved with hydrocyclone A. This result implies that hydrocyclone B, as compared to A was more efficient in removing particles. Despite the larger diameter of hydrocyclone B, higher efficiencies at similar Stokes' numbers can be partially attributed to a larger volume underflow receiver, which reduced the amount of particle reentrainment.

Using data collected with hydrocyclone A, an empirical equation was developed for the prediction of the gross removal efficiency as a function of the Stokes' number. This expression is represented by Eq. 3.

$$E_G = 1 - A * St^B \tag{3}$$

A and B are dimensionless constants. Other terms have been previously defined. Values of 0.018 and -0.64 were determined for A and B, respectively. The correlation coefficient for this fit was 0.74, and upper and lower 95% confidence values for B were -0.81 and -0.47, respectively. Since the greatest fraction of experimental data was for silica, a regression was also performed using only silica removal data. This resulted in values of 0.042 and -0.44 for A and B, respectively. The upper and lower 95% confidence values for B were -0.57 and -0.32, while the correlation coefficient was 0.84. Theoretical expressions developed for cyclones indicate that the fifty percent cut size (d_{50}) achieved is proportional to a Stokes' number raised to the -0.5 power (18). This cut size is directly proportional to the penetration. As a result, the value of B predicted by theory is -0.5. The theory which predicts this dependence, however, does not account for the presence of a batch underflow receiver.

The presence of a batch underflow receiver somewhat complicates the analysis of hydrocyclone efficiency data. Theoretical and empirical models are available for the prediction of hydrocyclone cut sizes, gross efficiencies, and pressure drops. However, these models do not incorporate an underflow receiver in their development. With an underflow receiver, phenomena such as reentrainment, flocculation of particles, and the accumulation of particles in the receiver over time affect the performance of the hydrocyclone. Furthermore, with changes in temperature and pressure, solubility effects can become significant. For removal to occur, a particle must be insoluble at the hydrocyclone entrance, centrifugally removed to the underflow receiver, and then settled in the underflow receiver before it can be reentrained. As a result of the complexity of such a system, there are no adequate theoretical models available for the prediction of operational parameters of a hydrocyclone with a batch underflow receiver.

Centrifugal Efficiencies/Cut Sizes

Particle size distributions were determined for all samples. These data were used to calculate cut sizes and for the development of grade efficiency curves. The cut size achieved by the hydrocyclone is the particle diameter for which a specific removal efficiency is achieved. For example, the fifty percent cut size (d_{50}) is that particle diameter for which 50% of particles (by number) are removed from the feed stream. Ninety (d_{90}) and ninety-five (d_{95}) percent cut sizes are analogously defined. Grade efficiency curves plot the removal efficiency of particles versus the particle diameter or the logarithm of the particle diameter. These show removal efficiencies achieved for all particle sizes detected.

Grade efficiencies, as shown in Figures 4 and 5, were achieved for silica particles with hydrocyclone A for two different mass flow rates at several temperatures. Grade efficiency curves with similar mass flow rates indicated increasing separation efficiencies of small particles with increased temperature. By comparison of Figure 4 with Figure 5, grade efficiencies also slightly increased with increasing flow rate. As displayed in Figure 6, zirconia, due to its increased density, exhibited higher removal efficiencies as compared to silica for the same size particles.

Unusual grade efficiency curves were observed for silica in experiments 4S-1 and 2 (70°C, 24.8 MPa). As shown in Figures 4 and 5, silica exhibited decreasing separation efficiencies to particles up to 2-3 μm in size, and increasing separation for particles above 3 μm in diameter. This trend in separation was observed in all silica experiments performed with an underflow receiver at temperatures below 100°C. Particle flocculation may have occurred. Small particles (0.5-1 μm) possibly combined to form larger particles (1-2 μm), which

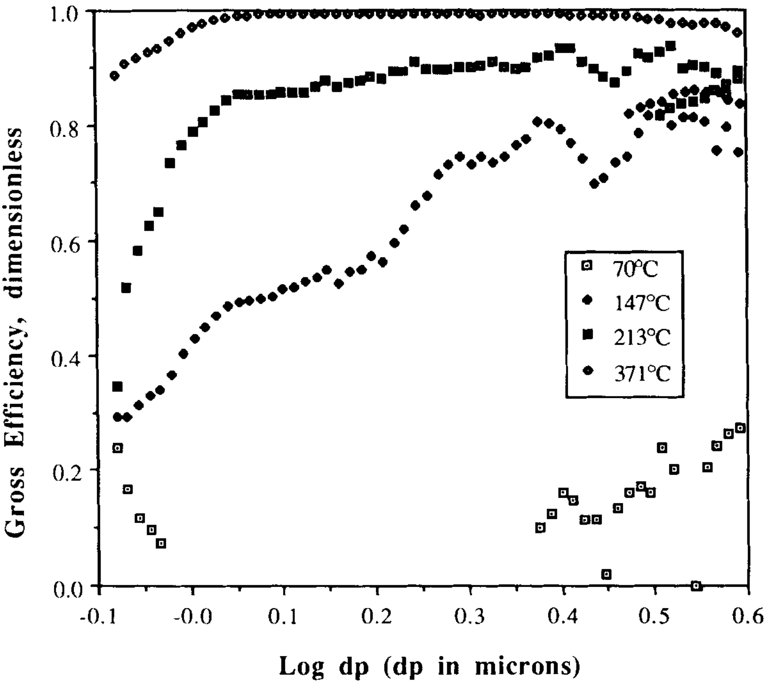

FIGURE 4. Grade efficiencies for silica experiments, 24.8 MPa, mass flow = 0.027 kg/s.

were not large enough to settle in the underflow receiver before becoming reentrained. Above a certain size (~3 μm), the particles avoided reentrainment and settled in the receiver.

Although the pH of zero point of charge (pH_{zpc}) is near 2.0 for silica at 20°C and atmospheric pressure (19), increased pressures appear to have elevated this pH_{zpc} to values near the feed pH (~6). Such a change would cause decreased particle stability and more favorable kinetics for Brownian flocculation in the underflow receiver (20). This may occur due to increased water densities in the particle's electric double layer, and a resulting neutralization of double layer charge. At higher temperatures, reduced water densities might reverse this effect, resulting in increased particle repulsion and decreased flocculation. The latter was observed experimentally.

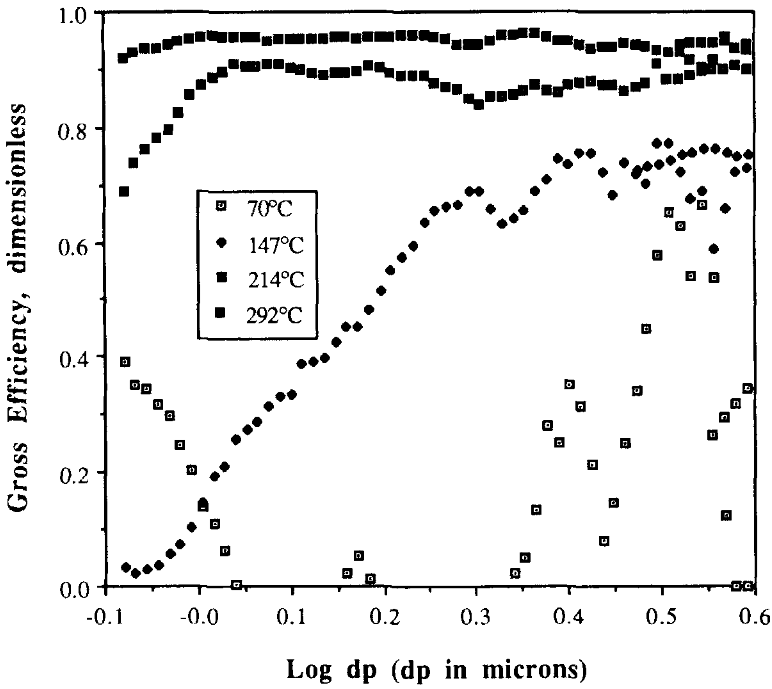

FIGURE 5. Grade efficiencies for silica experiments, 24.8 MPa, mass flow = 0.037 kg/s.

Cut sizes were determined from grade efficiencies. Due to the nature of grade efficiency curves, a single cut size (i.e. d_{50}) could not be determined for all experiments. As a result, values of d_{50}, d_{90}, and d_{95} are reported. A summary of cut sizes, as achieved with hydrocyclone A, is presented in Table 2. Cut sizes were smaller than previously reported for hydrocyclones. Values of d_{90} and d_{95} representing less than one µm were determined for several experiments. These values are typical of values achieved by efficient air cyclones.

For comparison with similar hydrocyclones, several experiments were conducted with hydrocyclone A at atmospheric pressure, room temperature, and without an underflow receiver. At a flow rate of 0.040 L/s, d_{50} values of 2.7 and 3.0 µm were determined. For comparison, Williamson and Bott (21), also using a 10 mm diameter hydrocyclone, found d_{50} values of 2.4 and 2.5 µm at a flow rate

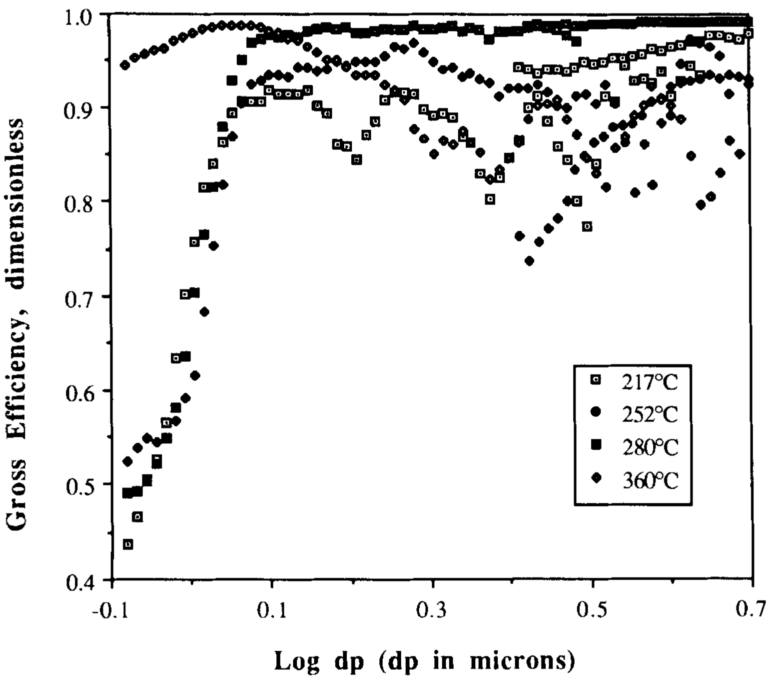

FIGURE 6. Grade efficiencies for zirconia experiments, 24.8 MPa, mass flow = 0.027 kg/s.

of 0.043 L/s for a quartz silica feed. Svarovsky (22) obtained d_{50} values of 2.2 and 2.5 μm for a chalk feed (s.g. = 2.78) with a 10 mm hydrocyclone at a flow rate of 0.40 L/s. Hydrocyclone A achieved similar cut sizes.

Underflow receiver size distributions assessed the concentrating effectiveness of the system, and determined the recovery of particle sizes. These data, plotted as the underflow to feed concentration ratio (U/F) versus the log of the particle diameter, are shown in Figure 7 for several experiments performed with silica. Increased concentration ratios are observed with increasing grade efficiencies (Figures 4 and 5). Particle balances confirmed the removal of particles by the hydrocyclone. For example, experiment 8T provided a U/F ratio of 62.4 for a two μm diameter particle (log dp = 0.3), while a U/F ratio of 62 was calculated from flow and grade efficiency data. Similar particle balances agree for

TABLE 2. SUMMARY OF CUT SIZE DATA*

Experiment	Particle	d50 (μm)	d90 (μm)	d95 (μm)
5T-1	SILICA	1.2		
5T-2	SILICA	1.6		
5T-3	SILICA	1.5		
5S-1	SILICA	2.4		
5S-2	SILICA	2.3		
5S-3	SILICA	2.0		
15T-1	TITANIA	1.0	1.6	
15T-2	TITANIA	1.3	2.4	
15T-3	TITANIA	1.2	1.9	
7T-3	TITANIA		1.7	1.8
8T-1	SILICA		1.8	
8T-2	SILICA		1.1	
8T-3	SILICA		1.6	
9T-1	ZIRCONIA		1.2	
9T-2	ZIRCONIA		1.1	1.8
9T-3	ZIRCONIA		1.1	1.9
10T-1	ZIRCONIA		1.2	1.2
10T-2	ZIRCONIA		1.2	1.7
10T-3	ZIRCONIA		1.1	1.4
11T-1	ZIRCONIA		1.4	1.7
11T-2	ZIRCONIA		1.1	1.7
11T-3	ZIRCONIA		1.1	1.2
6S-2	SILICA			1.2
6S-3	SILICA		0.8	1.0
12T-1	SILICA		0.9	1.0
12T-2	SILICA			1.0
12T-3	SILICA		0.9	1.0
13T-1	ZIRCONIA			0.9
13T-2	ZIRCONIA			0.8
13T-3	ZIRCONIA			0.8

*See Table 1 for experimental conditions. Experiments 15T-1,2, and 3 were carried out at 24.8 MPa, 20°C, at flow rates of 0.027, 0.037, and 0.047 kg/s.

experiments 5T and 8T. For experiments 4S and 4T, U/F ratios were below one up to particle sizes of 1.6 μm, and eventually rose to values of 10. Flocculation was indicated by U/F ratios less than one. The smallest particles were not accumulated in the underflow receiver because they formed larger particles which were subsequently reentrained or settled. This observation of flocculation agrees with the previously discussed behavior of grade efficiency curves.

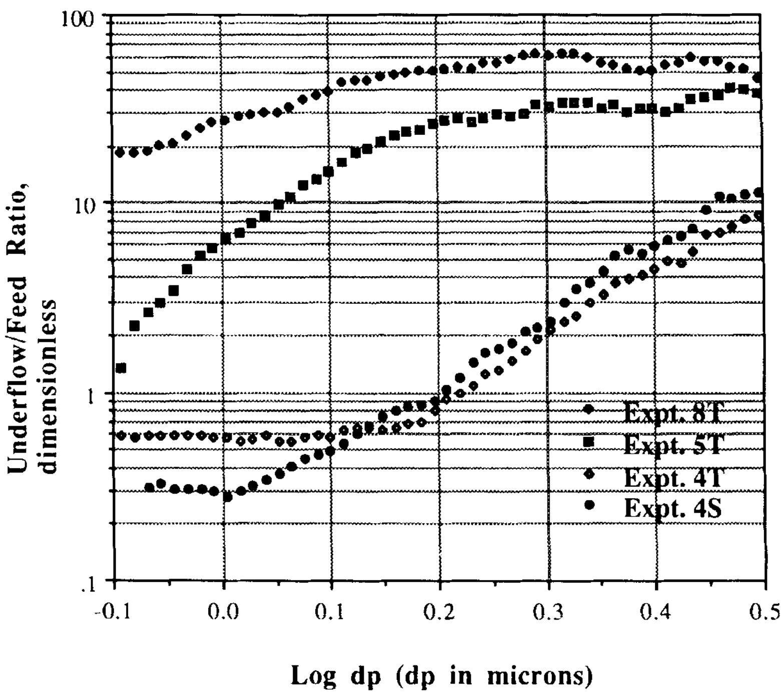

FIGURE 7. Underflow/feed ratio for silica experiments.

Pressure Drop

Pressure drop was measured at experimental conditions for both hydrocyclones. For hydrocyclone A, pressure drops varied from -34.5 kPa (20°C,0.027 L/s) to 758.5 kPa (360°C, 0.048 L/s). For hydrocyclone B, pressure drops ranged from 3.45 kPa (386°C, 0.0739 L/s) to 13.8 kPa (388°C, 0.119 L/s). Empirical models were developed for both hydrocyclones as a function of volumetric flow rate and viscosity. Multiple regressions with these variables led to the empirical expression depicted by Eq. 4:

$$\Delta P = K * Q^c * \mu^d \quad (4)$$

where

ΔP = pressure drop, Pa

Q = volumetric flow rate, L/s

K,c,d = constants determined by regression; c and d are dimensionless.

Two regression analyses were performed using hydrocyclone A pressure drop data, but only one analysis was performed using hydrocyclone B data. Two analyses were necessary for hydrocyclone A data due to different observed trends at low temperatures (< 250°C) and high temperatures (> 250°C). Low temperatures represented incompressible flow, while at high temperatures, a supercritical water phase in the heater provided the system with compressibility. The low temperature regression for hydrocyclone A yielded values of 1.62, 4.30, and -0.18 for K, c, and d, respectively. The high temperature analysis yielded values of 2940, 1.39, and 1.40 for K, c, and d. Finally, values of 2.45E+14, 2.75, and 2.14 were determined for K, c, and d for hydrocyclone B. Values of R^2 were 0.93, 0.84, and 0.85, respectively. Typically, values of c range from 2 to 3. Williamson and Bott determined a value of 0.101 for d (21). The latter values, however, are observed for hydrocyclones with no applied backpressure and without underflow receivers. These complications, along with the presence of a compressible phase, cause the exponents to differ.

CONCLUSIONS

Both hydrocyclones effectively removed micron-sized particulates from water streams at elevated temperatures and pressures. Gross removal efficiencies for quartz silica were as high as 80%, while such efficiencies for titania and zirconia exceeded 95%. An empirical expression was developed for predicting gross removal efficiencies of particulates achieved by a 10 mm diameter hydrocyclone with an underflow receiver. Grade efficiencies showed increased removal of all particle sizes with increased water temperatures. Cut sizes (d_{90} and d_{95}) below one micron were determined. Underflow receiver concentrations confirmed that particles were primarily removed by the hydrocyclone, and that there was little deposition on the walls of the apparatus. Pressure drops were also measured and modeled. For the 10 mm hydrocyclone, pressure drops ranged from -34.5 kPa (20°C,0.027 L/s) to 758.5 kPa (360°C, 0.048 L/s) for the ten mm hydrocyclone.

Similarly, for the 25.4 mm hydrocyclone, pressure drops ranged from 3.45 kPa (386°C, 0.0739 L/s) to 13.8 kPa (388°C, 0.119 L/s).

A small hydrocyclone with an underflow receiver, operating at high temperatures and pressures, was shown to be viable for solid-liquid separation. High gross efficiencies and low cut sizes for particles of known size distributions indicated that hydrocyclones should be effective in removing micron-sized particles from SCWO processes.

ACKNOWLEDGMENTS

This research was performed under appointment to the Environmental Restoration and Waste Management Graduate Fellowship Program, administered by Oak Ridge Associated Universities for the U.S. Department of Energy. Solids removal studies were made possible by equipment and staff provided by The University of Texas at Austin and Eco-Waste Technologies, Inc. The authors would like to thank Bob Cushing, Dennis Ku, Sarah Clark, and Dan Moran for their performance of particle size analyses.

REFERENCES

1. D.S. Lee, L. Li and E.F. Gloyna, J. Supercrit. Fluids. 3, 249 (1990).
2. T.B. Thomason and M. Modell, Haz. Waste. 1, 453 (1984).
3. M. Uematsu and E.U. Franck, J. Phys. Chem. Ref. Data. 9, 1291 (1980).
4. W.L. Marshall and E.U. Franck, J. Phys. Chem. Ref. Data. 10, 295 (1981).
5. E.U. Franck, Pure and App. Chem. 24, 13 (1970).
6. M.L. Japas and E.U. Franck, Ber. Buns. Phys. Chem. 89, 1268 (1985).
7. J.F. Connolly, AIChE J. 11, 13 (1966).
8. O.I. Martynova and O.K. Smirnov, Teploenergetika. 9, 145 (1964).
9. O.I. Martynova, in High Temperature, High Pressure Electrochemistry in Aqueous Solutions, NACE-4, 1976, p. 131.
10. P.A. Haas, E.O. Nurmi, M.E. Whatley, and J.R. Engel,"Hydraulic Cyclones For Application to Homogeneous Reactor Chemical Processing," ORNL-2301, U.S. Department of Energy, Oak Ridge, Tennessee, 1957.
11. F.C. Engel and J. Weisman, AIChE J. 6, 275 (1987).
12. W.R. Killilea, G. T. Hong, K.C. Swallow, and T.B. Thomason, SAE Tech. Paper Ser. No. 881038 (1988).
13. P.C. Dell'Orco, M.S. Thesis, Dept. of Civil Engineering, The University of Texas at Austin (1991).
14. F.J. Armellini and J.W. Tester, Proceedings of the 2nd International Conference on Supercritical Fluids. 21 (1991).
15. R. Parker, R. Jain, S. Calvert, D. Drehmel, and J. Abbott, Env. Sci. and Tech. 15, 451 (1981).
16. P.A. Patterson and R.J. Munz, Can. J. Chem. Eng. 67, 321 (1989).

17. G. Morey, Trans. ASME. 865, October (1951).
18. R.H. Perry and D.W. Green, Eds., Perry's Chemical Engineer's Handbook, 6th ed., McGraw Hill, New York (1984).
19. G.A. Parks and P.L. de Bruyn, J. Phys. Chem. 66, 967 (1962).
20. W. Stumm and J.J. Morgan, Aquatic Chemistry, John Wiley and Sons, New York (1981).
21. R.D. Williamson, T.R. Bott, H.S. Kumar, and I.H. Newson, Sep. Sci. and Tech. 18, 1395 (1984).
22. L.Svarovsky, in 2nd International Conference on Hydrocyclones, BHRA, 1984, p. 359.